

Examination of Photoluminescence Temperature Dependencies in N-B Co-doped 6H-SiC

V Gavryushin¹, K Gulbinas¹, V Grivickas¹, M Karaliūnas¹, M Stasiūnas¹,
V Jokubavičius², J W Sun², and M Syväjärvi²

¹Institute of Applied Research, Vilnius University, Saulėtekio av. 10, Vilnius, LT-10223 Lithuania

²Department of Physics, Chemistry and Biology, Linköping University, Linköping, SE-58183 Sweden

E-mail: vytautas.grivickas@ff.vu.lt

Abstract. Two overlapping photoluminescent (PL) bands with a peaks (half-width) at 1.95 eV (0.45 eV) and 2.15 eV (0.25 eV), correspondingly at 300 K, are observed in heavily B-N co-doped 6H-SiC epilayers under high-level excitation condition. The low energy band dominates at low temperatures and decreases towards 300 K which is assigned to DAP emission from the nitrogen trap to the deep boron (dB) with phonon-assistance. The 2.15 eV band slightly increases with temperature and becomes comparable with the former one at 300 K. We present a modelling comprising electron de-trapping from the N-trap, i.e. calculating trapping and de-trapping probabilities. The T-dependence of the 2.15 eV band can be explained by free electron emission from the conduction band into the dB center provided by similar phonon-assistance.

1. Introduction

Recently it was demonstrated that boron-nitrogen (B-N) co-doped 6H-SiC epilayers exhibits efficient donor-acceptor pair (DAP) light emission in a broad green-red spectral range [1-3]. Combining it with a common nitride based UV excitation from grown III-V nitrides on the top of 6H-SiC, this PL emission opens ability for a proper light conversion using a semiconductor as phosphor. In addition, PL emitted by Al-N DAP gives a broad blue-green spectral range and by assembling these two layers, the combination produces a white light emitting SiC source with high colour rendering parameters at room temperature (RT) [2].

Still, the PL emission mechanism itself, and particularly at the high co-doping, is not well understood. Up to now, very little is known on the donor-acceptor clustering, the deep defect structure and/or its modification with doping and how all these factors may influence the PL emission. In this work, the epitaxial heavily co-doped B-N thick 6H-SiC layers have been grown by sublimation growth process. The photoluminescence was studied at high injections which allowed total filling of the shallow and deep traps. We concentrated our study on the temperature and injection dependencies of the photoluminescence spectra in order to separate the main radiative emission components.

2. Samples and experimental techniques

The fast sublimation growth process was used to grow homoepitaxial co-doped layers on low-off axis 6H-SiC substrates. N and B were introduced via the controlled polycrystalline SiC source and the N concentration was also enhanced by the nitrogen gas ambient during the growth. In this work, two



samples both having a long carrier lifetime (detected in high injection up to ms-time range) were investigated. The sample ELS118 had epi-thickness $d = 45 \mu\text{m}$, the incorporated concentration N ($9.2 \times 10^{18} \text{ cm}^{-3}$), and B ($5.2 \times 10^{18} \text{ cm}^{-3}$). The sample ELS296 had the corresponding values of $d = 200 \mu\text{m}$, N ($1.2 \times 10^{19} \text{ cm}^{-3}$), and B ($2.1 \times 10^{18} \text{ cm}^{-3}$). The samples were placed in a close-cycle cryostat in a cold finger configuration and were excited with 355 nm 25 ps light pulses from a frequency tripled YAG laser which was operating at 10 Hz repetition rate. The excitation light penetration depth is about 11 μm and is nearly independent of temperature. The time-integrated PL was collected by a lens in 90° geometry, focusing the emission onto the entrance slit of the Hamamatsu spectrograph, while light detection was achieved through the intensified CCD-array. The spectral resolution was about 0.8 nm.

3. Experimental results and analysis

In figure 1a we plot the measured PL spectra from 8 K to 300 K with an increasing step from 5 K to 20 K. The constant injection fluence of 1.5 mJ/cm^2 was maintained during these measurements. The PL in the sample ELS118 is about 3-5 times higher than that in the sample ELS296 (note the difference in scale). Both samples emit in a similar broad range in which the PL maximum is shifting gradually to the blue wavelength from 680-705 nm to 590-580 nm with increasing temperature. At

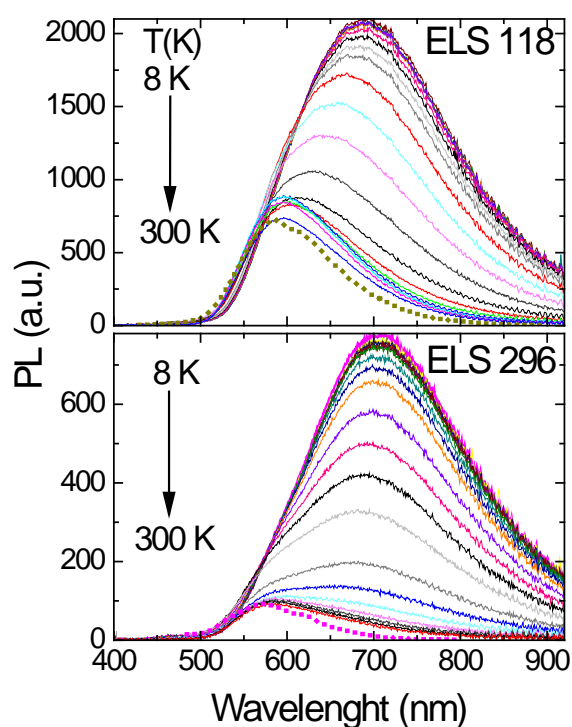


Figure 1a. PL spectra of two samples at different temperature. The excitation fluence is 1.5 mJ/cm^2 .

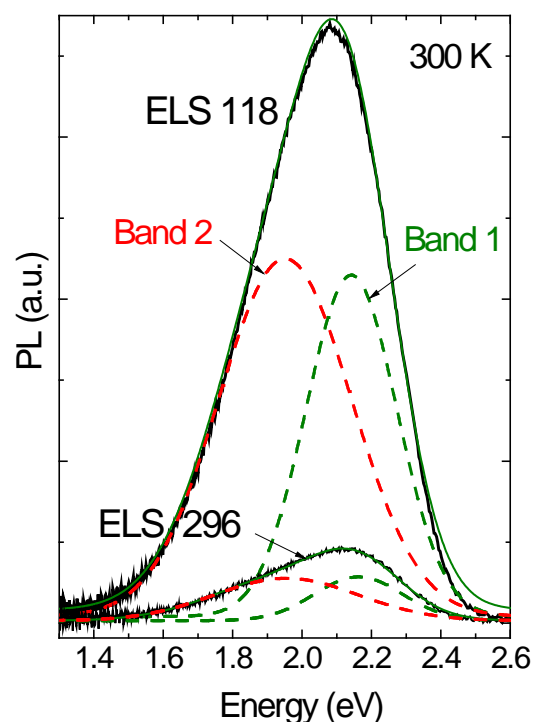


Figure 1b. Fitting of two Gaussian bands for PL spectrum of two samples at 300 K.

room temperature PL was measured also by an orders weaker cw-excitation, as reported in [2, 3]. The arbitrary normalized data are shown here by the dotted curves in figure 1a along with the high-injection data. Clearly, the high-injection RT PL data display substantial enlargement on the red emitted spectrum side. It is worth to note that for the cw-excitation a weaker shoulder was detected at 610-630 nm. Appearance of this shoulder has been attributed tentatively to the phonon-assisted replica in the N-dB DAP emission mechanism [2, 3]. For the high-injection conditions we did not record such

shoulder at any injection fluence which was varied between 0.025-2.5 mJ/cm². This absence can be explained by a fact that the shoulder is overwhelmed by an intensity enlargement on the red wavelength emission side.

The obtained higher temperature PL spectra (particularly in the ELS296 sample in figure 1a), appear to have a composition of two overlapping bands with a quite different temperature behaviour. In order to explore this behaviour, we have performed a fitting procedure of each PL spectrum using a free parameter variation by two Gaussian shapes. The fitting examples (hereafter denoted as “Band 1” and “Band 2”) are shown in figure 1b at 300 K. Obviously the corresponding sum of the two bands, as given by the fine line, exhibits a good first-rate agreement to the experimental data in both samples. The similar fit was achieved at other temperatures as well.

In figure 2a the fitting parameters are shown, i.e. the peak energies (E), the full-width half-maxima (FWHM) and the band amplitudes as a function of temperature. Solid symbols belong to the ELS118 and the open ones to the ELS296. The peak energy (FWHM) of the “Band 1” is 2.15 eV (0.45 eV) and the corresponding value of the “Band 2” is ~1.9 eV (0.25 eV). Peak energies E for the “Band 2” clearly shift towards high energy from 1.8 eV to 1.95 eV with rising temperature while for the “Band 1” a smaller shift is observed only for ELS118. The FWHM of both bands is slightly shrinking with T rising to 300 K. As can be noted from the lowest panel of figure 2a, the “Band 1” amplitude steeply decreases with T increasing and quite opposite trend is observed for the “Band 2”. Lastly, the amplitude increases with T for ELS118 or is about at a constant value for ELS296. In any case, the applicability of the two-band approach is appropriate above 100 K. At 300 K both bands are almost of the same amplitude. On the other hand, at $T < 50$ K, the “Band 2” alone can quite well represent the total PL spectrum. In figure 2b we show a single Gauss fit for the measured spectra at 8 K. The peak E is almost independent on the excitation fluence and the difference in the peak position is about 0.05 eV for both samples. However, the FWHM is slightly shrinking with increasing excitation fluencies. The PL amplitude increases linearly (a power factor 1.0) at low fluencies. At higher fluencies above 0.5 mJ/cm² it tends to saturate. More than an order lower emission was resolvable in the ELS118 sample spectrum at 8 K in the high energy range between 2.6-2.8 eV, i.e. closer to the band edge. Its intensity dependence is presented in the lower panel of figure 2b, which shows that this emission is saturated at 0.2 mJ/cm². PL emission in this range can be caused by non-intentional Al acceptor through Al-N DAP mechanism. To summarize the obtained results we derive that all available traps are perhaps under saturation at 1.5 mJ/cm². The estimated injected pair density at the absorption depth for this fluence is at about 10^{19} cm⁻³.

Since the deep boron (dB) with energy ~550-750 meV is the dominant acceptor impurity in the investigated epilayer [1], the electron emission from nitrogen trap to the deep boron, i.e. DAP emission could be related to the “Band 2”. On the other hand, the “Band 1” which intensity increases with T , can be assigned to the emission of free-electron transition to the deep boron. According to Thomas et al. [6], the energy of DAP recombination is given in first approximation by the equation: $E(r) = E_g - (E_a + E_d) + e^2/\epsilon r$ where E_g is the band gap energy; E_a and E_d are the ionization energies of acceptor and donor; ϵ is the dielectric constant. Electron and hole pairs located in a close lattice sites present the strongest coulomb interaction and their recombination results in emission of larger energy photons contributing to the blue side of the DAP band [6]. The energy of phonons emitted by infinitely distant pairs is $E(\infty) = E_g - (E_a + E_d)$. Therefore, emission from DAP “Band 2”, estimating $E_g = 2.95$ eV, $E_a = 0.65$ eV, $E_d = 0.1$ eV, would account for $E > 2.2$ eV. For the case of emission from conduction band-to-dB (for “Band 1”) it should be set $E_d = 0$ eV which corresponds to emission at $E > 2.3$ eV. Both approaches cannot account for the low energy side of observed PL bands. Thus, in the DAP recombination model it should be pointed out that either a large energy is taken by the phonons for the indirect bandgap SiC or the impurities are distributed in a wide energy range within the band gap. An alternative approach could be excitonic recombination mechanisms at the deep trap but this mechanism is unlikely at high-injection conditions.

In figure 3a the Arrhenius plot for the the amplitude of “Band 2” in both samples is shown. Excluding the high T range of the sample ELS118, we may estimate a trend from the PL slope that an

activation energy of the trap is 53 meV. This value is in a perfect agreement to the same value deduced for the hundred- μ s-long electron lifetime component in the sample ELS118 [see Manolis et al. this issue].

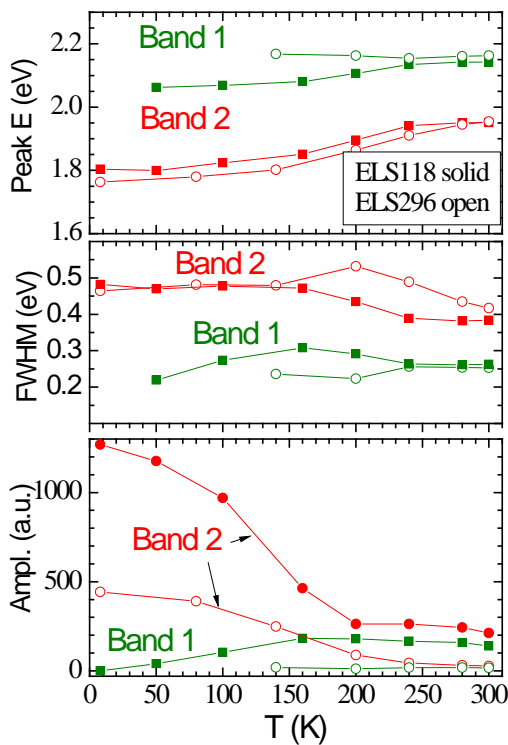


Figure 2a. T-dependencies of “Band 1” and “Band 2” peak energy, FWHM and the relative amplitudes at the excitation fluence of 1.5 mJ/cm².

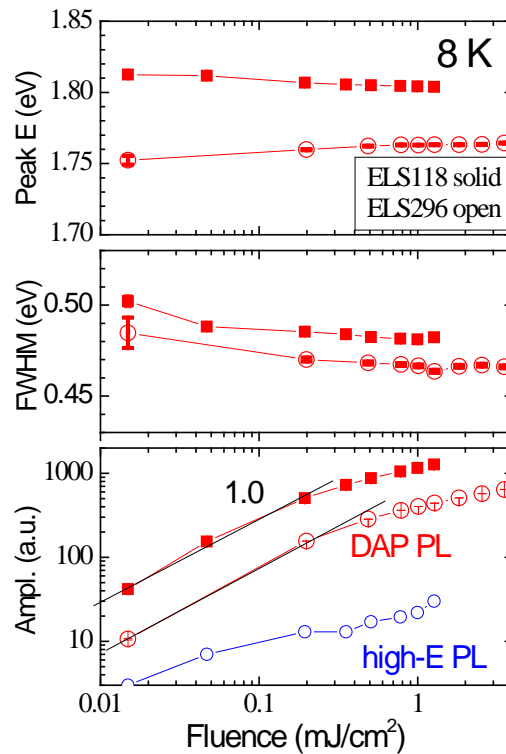


Figure 2b. The dependences on fluence of PL peak energy, FWHM and the amplitude in two samples at 8 K (a Gauss fit corresponds to the “Band 2”).

Concerning the basic assumption for two band model, we provide a carrier population calculation. The calculation is based on a simple recombination model consisting of one trapping and one recombination center for the excess electrons. We solved a set of coupled rate equations for the free electrons $n(t, T)$, trapped electrons $n_t(t, T)$, and electrons captured by recombination centers $n_r(t, T)$, like in a model presented by Ichimura [7]. Thermal velocity, ionization rates and the effective density of states in the conduction band were taken with a 200- μ s long recombination lifetime and the capture cross-section for the neutral-charged N-trap was fixed at the typical value of $\sigma_n^t = 2 \cdot 10^{-17}$ cm². Then, we calculated carrier occupation in the N-trap and in the conduction band at quasi-thermodynamic equilibrium after the excitation pulse. Calculation was performed for trap levels E_t in the range from 10 meV to 100 meV at different temperatures. A plot in figure 3b shows two curve sets that are applied to the PL results for the “Band 2” and the “Band 1”. The experimental points are taken from ELS118 sample of figure 2a. Carrier density in the N-trap (solid curves) was arbitrarily adjusted at the low temperature to the experimental PL amplitude value of 1280 (a.u.). A family of carrier densities in the conduction band (dashed curves) was adjusted to the N-trap value by multiplying the calculated result by the factor $\times 0.4$, i.e. assuming slightly reduced emission probability. The dashed-dotted line in figure 3b shows the T-dependence in the case of no trap levels $N_t = 0$. In total, figure 3b plot reveals that occupation of N-trap and the conduction band can satisfactorily explain both PL band T-dependencies. The estimated thermal activation energy of N-trap is, however, lower, perhaps $E_t \approx 10$ -

20 meV. The substantial deviation of experimental point from the curves occurs at $T > 150$ K. This can be explained by the fact that radiation emission probability was taken as a constant value, without taking into account the increase of phonon density. In order to verify this hypothesis, a proper mechanism for phonon-assistance in PL emission mechanism should be developed.

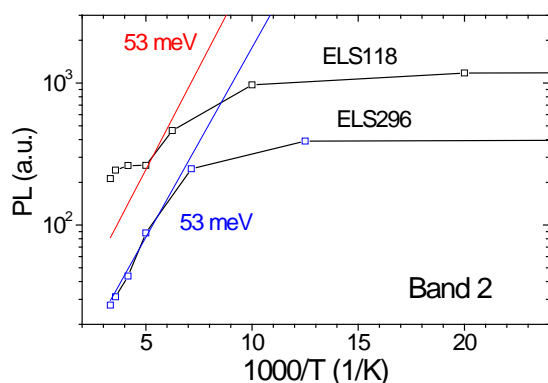


Figure 3a. Arrhenius plot of PL for the amplitude of the “Band 2”.

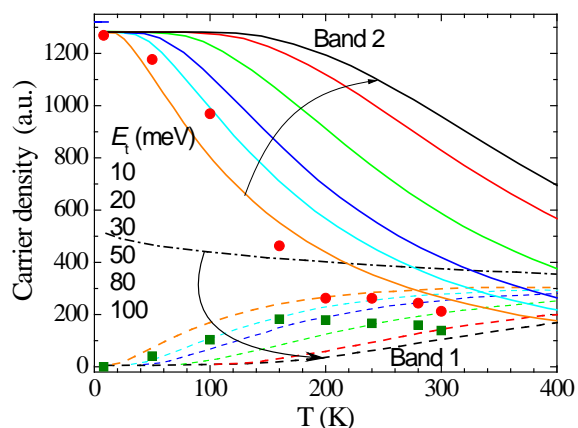


Figure 3b. T-dependencies of the electron density in the conduction band (Band 1) and in the N-trap (Band 2) at different trap energies. The experimental points are taken for ELS118 sample.

4. Conclusions

By applying PL measurements at high-injection levels we have shown that PL emission spectra are composed of two distinct broad bands “Band 1” and “Band 2” with a strictly different T-dependency. The RT PL data display substantial enlargement on the red emitted spectra side in respect to low cw-excitation spectra. This effect can be attributed to the enhanced phonon-assistance at high excitation. The low energy band we relate to the phonon-assisted N-dB DAP radiation with a thermal activation energy of 53 meV which is assigned for the N-trap. While the high energy band component is attributed to the phonon-assisted free-electron radiation recombination from the conduction band into the dB trap. The general behaviour of the T-dependencies in PL bands is basically governed by the occupation probability of the N-trap.

References

- [1] Kamiyama S, Maeda T, Nakamura Y, Iwada M, Amano H, Akasaki I, Kinoshita H, Furusho T, Yoshimoto M, Kmoto T, Suda J, Henry A, Ivanov I G, Bergman J P, Monemar B, Onuma T and Chichibu S F 2006 *J. Appl. Phys.* **99** 093108
- [2] Syväjärvi M, Müller J, Sun J W, Grivickas V, Ou Y, Jokubavicius V, Hens P, Kaisr M, Ariyawong K, Gulbinas K, Liljedahl R, Linnarsson M K, Kamiyama S, Wellmann P, Spiecker E and Ou H 2012 *Physica Scripta* **T148** 014002
- [3] Sun J W, Jokubavicius V, Liljedahl R, Yakimova R, Juillaguet S, Camassel J, Kamiyama S and Syväjärvi M 2012 *Thin Solid Films* **522** 33-35
- [4] Duijn-Arnold A V, Icoma T, Poluektov O G, Baranov P G, Mokhov E N and Schmidt J 1998 *Phys. Rev. B* **57** 1607-19
- [5] Lebedev A 1999 *Semiconductors* **33** 107-30
- [6] Thomas D G, Hopfield J J and Augustyniak W M 1965 *Phys. Rev.* **140** A202-220
- [7] Ichimura M 2006 *Solid-State Electronics* **50** 1761-6